Infection and Drug Resistance

Dovepress
Taylor & Francis Group

Open Access Full Text Article

ORIGINAL RESEARCH

COMMD1 Regulates Osteoclast Differentiation in Talaromyces marneffei-Induced Osteomyelitis via the NF-κB Pathway

Yi Zhang[1,*], Fayun Yang[1,*], Weilun Zhao[2], Rufei Wei[3], Gaofeng Zeng[3], Shaohui Zong[1,4]

[1]Department of Spine Osteopathia, The First Affiliated Hospital of Guangxi Medical University, Nanning, Guangxi, 530021, People's Republic of China; [2]Collaborative Innovation Centre of Regenerative Medicine and Medical BioResource Development and Application Co-constructed by the Province and Ministry, Guangxi Medical University, Nanning, Guangxi, 530021, People's Republic of China; [3]School of Public Health, Guangxi Medical University, Nanning, Guangxi, 530021, People's Republic of China; [4]Wuming Hospital of Guangxi Medical University, Nanning, Guangxi, 530021, People's Republic of China

*These authors contributed equally to this work

Correspondence: Shaohui Zong, Department of Spine Osteopathia, The First Affiliated Hospital of Guangxi Medical University, No. 6 Shuangyong Road, Qingxiu District, Nanning, Guangxi, 530021, People's Republic of China, Email zongshaohui@gxmu.edu.cn; Gaofeng Zeng, School of Public Health, Guangxi Medical University, No. 22, Shuangyong Road, Qingxiu District, Nanning, Guangxi, 530021, People's Republic of China, Email zenggaofeng@gxmu.edu.cn

Purpose: This study investigated the role of copper metabolism MURR1 domain-containing 1 (COMMD1) in Talaromyces marneffei (TM)-induced osteomyelitis (OM) and its regulation of osteoclast differentiation via the NF-κB pathway.

Methods: A murine TM infection model was used to assess bone destruction and osteoclast activity via micro-CT, histological analysis, biomechanical testing, qPCR, and Western blot. RNA sequencing was performed to analyze differentially expressed genes. Functional validation was conducted using COMMD1 conditional knockout (cKO) mice and bone marrow-derived monocytes macrophages (BMMs). The NF-κB inhibitor JSH-23 was used to verify pathway dependency.

Results: TM infection significantly upregulated inflammatory cytokines (IL-10, IL-17, TNF-α) and induced severe bone structural damage, characterized by trabecular thinning and reduced mechanical strength. These changes were accompanied by increased osteoclast numbers and elevated expression of osteoclast differentiation-related genes (TRAP, NFATc1, Ctsk, FOS). RNA sequencing revealed downregulation of COMMD1 and activation of the NF-κB pathway in TM-infected mice. COMMD1 deficiency exacerbated bone destruction and osteoclast differentiation, while COMMD1 overexpression suppressed these effects. Mechanistic studies showed that COMMD1 deletion increased P65 phosphorylation and decreased IκBα expression, effects that were reversed by JSH-23 treatment.

Conclusion: COMMD1 protects against TM-induced OM by inhibiting the NF-κB pathway, suggesting it as a potential therapeutic target for bone infections.

Keywords: Talaromyces marneffei, COMMD1, osteomyelitis, osteoclast differentiation

Introduction

Osteomyelitis (OM) refers to a bone disease characterized by inflammation due to microbial pathogen invasion, with *Staphylococcus aureus* being the most common causative agent.[1,2] Based on the route of infection, OM can be classified into hematogenous, contiguous, and post-traumatic types, among the various forms of OM, post-traumatic cases dominate, comprising around 80% of incidences. It is frequently associated with open fractures or postoperative infections.[3] The pathogenesis of OM is complex, involving inflammatory responses, bone destruction, and an imbalance in bone remodeling.[4] Early diagnosis combined with appropriate antibiotic therapy can effectively treat acute OM. However, chronic OM is often accompanied by bone loss, localized ischemic sclerosis, and impaired soft tissue regeneration, rendering systemic antibiotics alone insufficient for effective treatment.[5] The appearance of bacteria with resistance to antibiotics, driven by prolonged overuse in recent years, has further impaired clinical efficacy.[6,7] Moreover, OM is characterized by a prolonged treatment

Received: 4 June 2025
Accepted: 24 October 2025
Published: 21 November 2025

course and a high recurrence rate, which severely compromises patients' well-being and contributes to significant strain on healthcare services and broader economic systems.[8]

Talaromyces marneffei (TM) is a dimorphic mushroom primarily indigenous to southern China and Southeast Asia. TM typically leads infections in the lungs, skin, and lymphatic system.[9–11] In recent years, studies have reported that TM can also involve bone tissue, leading to severe complications such as OM.[12] Compared with other pathogenic fungi, such as Histoplasma or Coccidioides, bone infections have been reported, typically presenting as osteolytic lesions and chronic granulomatous inflammation in disseminated disease. However, these cases are largely confined to specific endemic regions and are relatively well recognized clinically.[13–15] In contrast, bone infections caused by Talaromyces marneffei are rare, often accompanied by severe bone destruction, and remain poorly understood with limited diagnostic guidance. The challenges of difficult diagnosis and complex treatment further complicate clinical management.[16] In-depth investigation into the pathogenic mechanisms of TM-induced bone infections is essential for improving the recognition and management of TM-related bone damage, thereby enhancing patient outcomes and reducing both disability and mortality rates.

COMMD1 (copper metabolism MURR1 domain-containing 1) is a multifunctional intracellular protein initially identified for its role in copper homeostasis. Subsequent studies have demonstrated that it also plays important roles in protein degradation, signal transduction, and inflammatory responses, making it a key regulator of immune homeostasis and inflammatory signaling pathways.[17,18] Studies have shown that downregulation of COMMD1 expression increases the sensitivity of certain tumor cells, such as SAS and H460 cells, to inflammatory stimuli. Additionally, it suppresses the responsiveness of macrophages and cancer cells to tumor necrosis factor-alpha (TNF-α) and interleukin-1 (IL-1), thereby exacerbating inflammatory reactions.[19] Notably, COMMD1 functions as a hypoxia-sensitive negative regulatory factor that integrates signal transduction and metabolic activities within human macrophages, thereby inhibiting osteoclastogenesis. Specifically, COMMD1 modulates osteoclast differentiation by suppressing the RANKL- driven NF-κB signaling pathway and the E2F1-dependent metabolic pathway.[20] In addition, other members of the COMMD protein family have also been found to be closely involved in immune regulation and bone metabolism. COMMD3 can regulate copper metabolism through the ATOX1–ATP7A–LOX axis, thereby promoting the progression of multiple myeloma.[21] Nevertheless, existing studies have mainly focused on tumor-related inflammatory mechanisms, the role and underlying mechanisms of COMMD1 in orthopedic infectious diseases remain poorly understood and warrant further investigation.

This study explores the function and underlying mechanism of COMMD1 in TM-induced OM, particularly its regularization of NF-κB signaling in the inhibition of osteoclast differentiation. By constructing a TM infection model in mice, this research explores COMMD1's regulatory impact on bone metabolism and its value in guiding early diagnostic and therapeutic strategies for TM-related OM.

Materials and Methods

Murine Osteomyelitis Model

To establish a murine model of OM, 6–8-week-old C57BL/6N mice were used. Under anesthesia with sodium pentobarbital, a skin incision was made over the right hind limb to expose the tibial surface. A central hole (approximately 1 mm in diameter) was drilled into the tibia using a high-speed micro-drill. Subsequently, 10 μL of TM bacterial solution (1×10^8 CFU/mL) was implanted into the bone marrow chamber. The bone defect was sealed with bone wax, and the overlying soft tissues, including muscle and skin, were closed in layers. Mice were humanely euthanized 14 days following surgical intervention, and their tibiae were collected for subsequent analysis. Based on the experimental treatment, mice were stochasticly assigned to three groups (n = 5 per group): control, TM-infected, and TM infection with COMMD1 conditional knockout (cKO) group. The cKO mice were obtained from Cyagen Biosciences. The Animal Ethics Committee of Guangxi Medical University approved the experimental protocol for this study (NO. 202210014).

Cell Culture and Treatment

Cells from the bone marrow were obtained by harvesting tibiae from C57BL/6N mice. After removing both ends of the tibiae, single-cell suspensions were prepared by irrigating the bone marrow chamber with culture medium delivered via syringe. Cells were filtered using a 70 μm mesh, centrifuged, and resuspended in α-MEM medium enriched with 10%

FBS (C04001-050, VivaCell Biosciences) and 1% penicillin–streptomycin (4014, Servicebio), followed by incubation at 37 °C in a humidified 5% CO_2 incubator. Twenty-four hours post-incubation, unattached cells were removed, and the remaining adherent population was collected as bone marrow-derived macrophages (BMMs).[22,23]

The BMMs were then infected with TM for 7 days to induce OM. To determine the role played by NF-κB signaling, a 24-hour treatment with JSH-23 (10 μM), a selective NF-κB inhibitor, was applied to the cells.

Cell Transfection

To develop a vector for COMMD1 overexpression, the COMMD1 gene sequence was cloned from a COMMD1 expression plasmid (Sangon Biotech, ABX42471-1) and inserted into the pEGFP-N1 vector at the NheI and AgeI restriction sites. Subsequently, the empty vector or the COMMD1 overexpression plasmid was transfected into cells using Lipo8000 transfection reagent (Beyotime, C0533) for subsequent experimental analyses.

Micro-Computed Tomography (Micro-CT)

After removal of muscle and soft tissue, a 48-hour fixation in 4% paraformaldehyde was applied to the tibiae. Mimicro-CT imaging was then performed using a SkyScan 1276 scanner (Bruker). With parameters set at 70 kV and 200 μA, scanning was completed, and image datasets were reconstructed via NRecon. Quantification of the acquired scans was achieved using CTAn.

Quantitative Real-Time Polymerase Chain Reaction (qRT-PCR)

The connective tissue surrounding the tibia was carefully removed, and the bone was immediately placed in RNA preservation solution (Invitrogen). The tissue was then pulverized into a fine powder under liquid nitrogen. In line with the manufacturer's protocol, total RNA was obtained through TRIzol reagent (Invitrogen) and subsequently used for cDNA synthesis. qPCR was executed with the SYBR Green Master Mix (ZA303-101S, GeneSTAR) on the StepOnePlus system (Applied Biosystems). qPCR was carried out beginning with an initial denaturation phase of 5 minutes at 95°C, followed by 40 cycles of 95°C for 15 seconds and 60°C for 30 seconds for annealing and extension. To determine relative mRNA levels, the $2^{-\Delta\Delta Ct}$ method was applied. The sequences of the primers are listed below:TRAP, Forward: 5′-ACACAGTGATGCTGTGTGGCAACTC-3′; Reverse: 5′-CCAGAGGCTTCCACATATATGATGG-3′; FOS, Forward: 5′-CCAGTCAAG-AGCATCAGCAA-3′; Reverse: 5′-AAGTAGTGCAGCCCGGAGTA-3′; NFATc1, Forward: 5′-GGTGCTGTCTGGCCATAACT-3′; Reverse: 5′-GAAACG CTGGTACTGGCTTC-3′; Ctsk, Forward: 5′-GCTTGGCATCTTTCCAGTTTTA-3′; Reverse: 5′-GCTCAGTAA-CAGT CCGCCTAGA-3′.

Western Blotting

RIPA buffer with protease inhibitors was used to lyse tibial tissues and extract total proteins, which were then quantified using the BCA kit (P0010S, Beyotime). Protein samples were mixed with SDS loading buffer, separated on 10% SDS-PAGE gels, and subsequently blotted onto PVDF membranes. Membranes underwent a 1-hour blocking step in 5% BSA at ambient temperature, then were incubated overnight at 4°C with primary antibodies, and finally treated with HRP-conjugated secondary antibodies for 1 hour the next day. Detection was carried out using the ECL kit (BL520B, Biosharp), and signals were recorded using a gel imaging system. To ensure consistency, band intensities were normalized using β-actin as the housekeeping protein. The antibodies used are as follows: NFATc1 (1:1000, ab25916, Abcam); Ctsk (1:500, 57056, CST); FOS (1:1000, ab222699, Abcam); P-P65 (1:1000, 3033, CST); β-actin (1:4000, 20536-1-AP, Proteintech); P65 (1:1000, 10745-1-AP, Proteintech); COMMD1 (1:500, 11938-1-AP, Proteintech); IκBα (1:5000, 10268-1-AP, Proteintech).

Enzyme-Linked Immunosorbent Assays (ELISA)

To obtain serum, blood was drawn and kept at room temperature for 2 hours to facilitate clotting, then subjected to centrifugation at 3000 rpm for 15 minutes at 4°C. The concentrations of IL-10, IL-17, and TNF-α in the serum were measured using commercial ELISA kits, following the manufacturers' instructions for all procedures, The optical density at 450 nm was determined with a microplate reader. (Thermo Fisher Scientific, USA).

Histological Analysis

Tibiae were harvested from mice and decalcified in a solution containing EDTA and glycerol at 4°C for 5–7 days. After decalcification, tissues were processed through conventional dehydration steps and embedded in paraffin. A rotary microtome was employed to prepare 5 μm-thick tissue slices.[24] Histological specimens were subsequently treated with hematoxylin and eosin (H&E) and TRAP staining to evaluate bone structure and osteoclast function.

Phalloidin Staining

BMMs obtained from the control group, TM-infected group, Cells from the TM-infected COMMD1 cKO group were cultured in 96-well plates (5×10^3/well) and maintained in a medium containing M-CSF (30 ng/mL) and RANKL (50 ng/mL) for 7 days to urge osteoclastogenesis. After incubation, fixation was done with 4% paraformaldehyde for 30 minutes, followed by 10-minute permeabilization using PBS plus 0.1% Triton X-100. Samples were incubated with 3% BSA in PBS for 1 hour at room temperature to minimize non-specific binding. Cells were gestated with Phalloidin in the dark at 37°C for 1 hour, then stained with DAPI to mark nuclei. Following PBS washes, fluorescence imaging was carried out on an EVOS confocal microscope, and the images were evaluated through the designated analysis software.

TRAP Staining

BMMs (5×10^3 cells/well) were plated in 96-well plates and cultured for 7 days in medium supplemented with M-CSF (30 ng/mL) and RANKL (50 ng/mL). Cells were defiled for TRAP based on the kit's instructions to measure TRAP enzymatic activity. Cells exhibiting positive TRAP staining and harboring no fewer than three nuclei were classified as osteoclasts.

Biomechanical Analysis

After dissection, mouse tibiae were carefully cleaned of surrounding soft tissues and subjected to three-point bending tests using the Instron 5685 mechanical testing system. All tests were conducted under constant temperature and humidity conditions. For testing, the right tibia was placed horizontally on two support points with a span of 15 mm, ensuring that the long axis of the tibia was perpendicular to the loading axis and the midpoint aligned with the span center. A cylindrical loading head (1 mm diameter) applied a downward vertical force at a speed of 0.01 mm/s until fracture occurred. Load and displacement data were recorded every 0.1 second to generate load–displacement curves, from which mechanical parameters including elastic modulus, maximum load, fracture load, elastic load, and bending energy absorption were calculated.

For compression testing, the distal end of each specimen was secured in the testing device and positioned on the compression platform. Compression was implemented at a consistent velocity of 5 mm/min until the specimen fracture. The system recorded parameters including maximum load, stress, displacement, and strain. Calculation of the elastic modulus was based on the initial linear region of the stress–strain plot.

RNA-Sequencing

RNA sequencing was performed by Novogene, using samples derived from control and TM-infected mice. TopHat was used to align the raw sequencing reads to the mm9 mouse reference genome. Normalization of library read counts was conducted using a scaling factor in the edgeR package prior to differential expression analysis. Differentially expressed genes (DEGs) with the DEGSeq R package (v1.20.0), followed by P-value correction using the Benjamini-Hochberg procedure. Significant differential expression was defined as $|\log_2 \text{fold change}| > 1$ with a q-value less than 0.005. Enrichment analysis for DEGs was conducted via the clusterProfiler package in R.

Statistical Analysis

All data are shown as mean values with corresponding standard deviations (SD). The normality of data distribution was assessed using the Shapiro–Wilk test. For normally distributed data, Two-group comparisons were conducted using the independent samples *t*-test, whereas group differences involving three or more sets were assessed via one-way ANOVA.

All statistical analyses were conducted using SPSS software (version 23.0, IBM, USA), and a p-value < 0.05 was considered statistically significant.

Results

TM Infection Induces Inflammatory Response and Body Weight Loss

After establishing the OM mouse, serum concentrations of IL-10, IL-17, and TNF-α were quantified by ELISA. Relative to the control group, these cytokines exhibited a marked elevation in the TM-infected group ($p < 0.05$) (Figure 1A–C). During the infection period, mice in the TM group exhibited progressive weight loss, demonstrating a notable decrease on day 14 ($p < 0.05$) (Figure 1D). Bone marrow cultures from tibias collected on day 14 confirmed TM positivity (Figure 1E).

TM Infection Leads to Significant Bone Damage

To evaluate the effect of TM infection on the skeletal structure and mechanical strength in murine models, tibial samples were collected 14 days post-infection for histological staining, biomechanical testing, and micro-CT analysis. H&E staining demonstrated that trabecular bone in the TM-infected group exhibited disrupted architecture, with sparsely arranged and fractured trabeculae accompanied by inflammatory cell infiltration (Figure 2A). TRAP staining indicated a marked elevation in osteoclast number and activity within the TM group (Figure 2B).

In the three-point bending test, the elastic modulus, maximum bending stress, and fracture-point force of the tibiae showed a significant reduction in the TM group relative to the control group ($p < 0.05$) (Figure 2C). Compression testing further demonstrated a marked reduction in both maximum load and compressive elastic modulus in the TM group ($p < 0.05$) (Figure 2D), indicating compromised resistance to mechanical stress.

Micro-CT three-dimensional reconstruction revealed substantial TM-induced bone structural damage (Figure 2E). Quantitative analysis exhibited no meaningful variation in total tissue volume (TV); however, the TM group exhibited significantly reduced trabecular thickness (Tb.Th), increased trabecular separation (Tb.Sp), decreased trabecular number

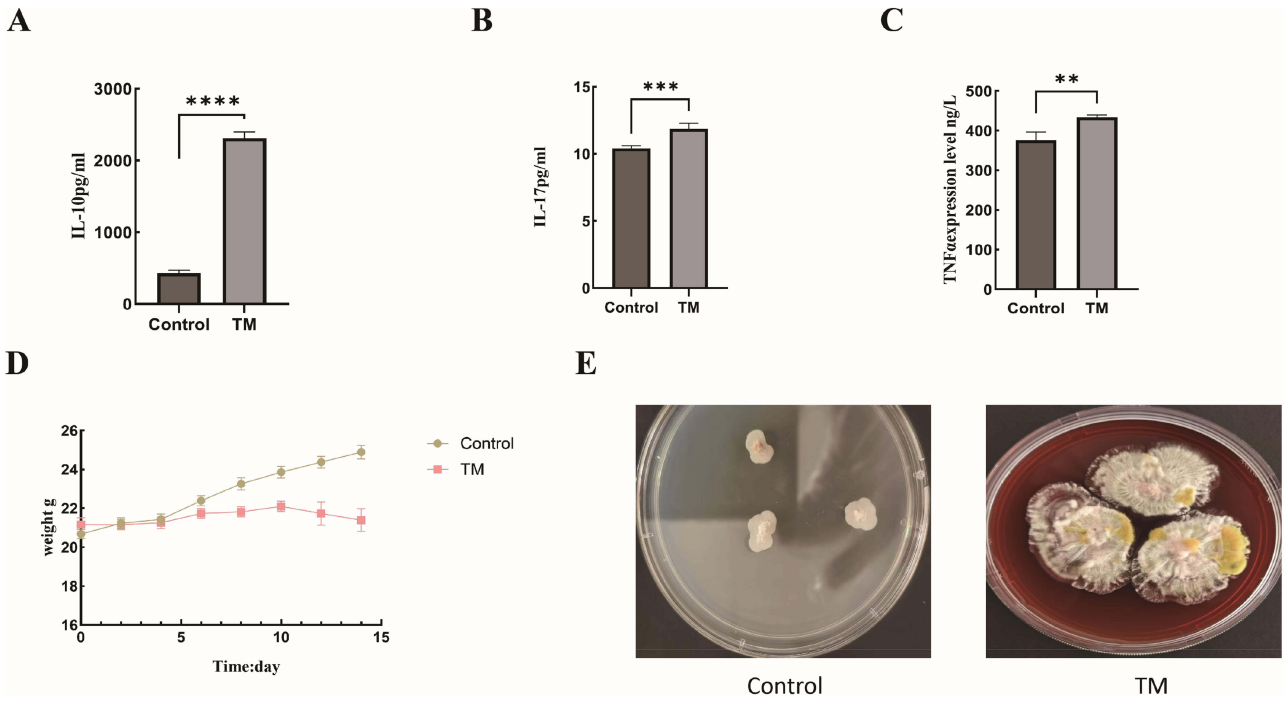

Figure 1 Talaromyces marneffei (TM) infection induces elevated inflammatory cytokine levels and body weight loss in mice. (**A**–**C**) ELISA results showing significantly increased serum levels of IL-10, IL-17, and TNF-α in TM-infected mice compared to controls. (**D**) Continuous monitoring of weight changes over a 14-day period in TM-infected mice compared to control mice. (**E**) Fungal culture of tibial bone marrow at day 14 on potato dextrose agar (PDA) medium revealed TM colony growth in the TM-infected group, whereas no colonies were observed in the control group. n=5. **$p < 0.01$, ***$p < 0.001$, ****$p < 0.0001$ vs Control group.

https://doi.org/10.2147/IDR.S544816

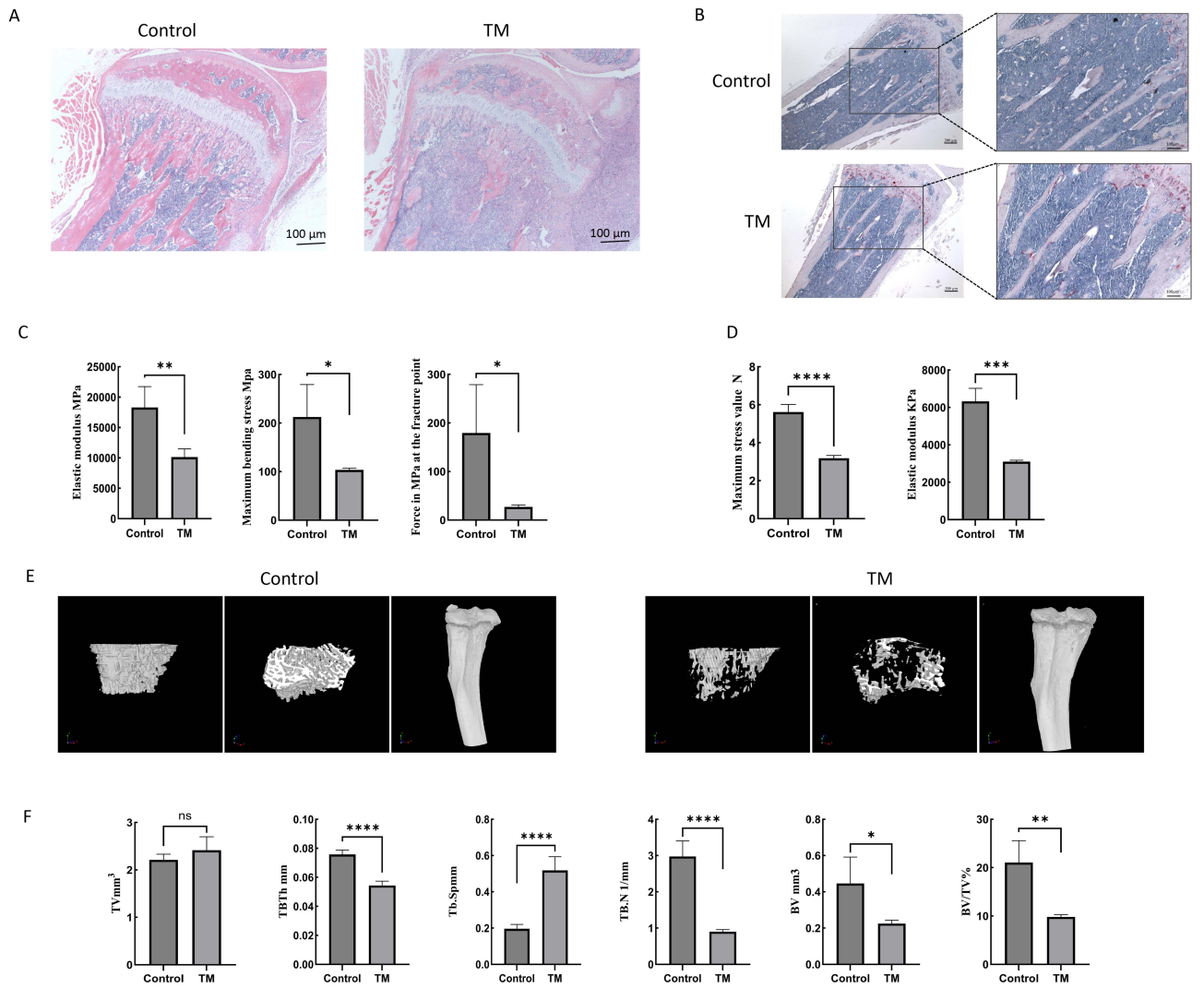

Figure 2 TM infection induces bone destruction, mechanical weakening, and trabecular deterioration in mice. (**A**) H&E staining shows disrupted trabecular structure and inflammatory infiltration in TM-infected tibiae. (**B**) TRAP staining reveals increased osteoclast number and activity in the TM group. (**C**) Three-point bending and (**D**) compression tests demonstrate reduced mechanical strength in TM-infected bones. (**E**) Micro-CT 3D reconstruction reveals structural damage in TM-infected tibiae; Axes x, y, and z represent the three-dimensional orientation (x: left–right; y: anterior–posterior; z: superior–inferior) in micro-CT analysis. (**F**) Quantitative analysis shows decreased trabecular thickness (Tb.Th), increased separation (Tb.Sp), decreased trabecular number (Tb.N), reduced bone volume (BV) and bone volume fraction (BV/TV), with no significant change in total volume (TV). n=5. *$p < 0.05$, **$p < 0.01$, ***$p < 0.001$, ****$p < 0.0001$ vs Control group.

(Tb.N) and (BV), as well as a lower bone volume fraction (BV/TV) ($p < 0.05$) (Figure 2F), indicating severely impaired trabecular quality and structural integrity.

TM Infection Enhances Osteoclast Differentiation and Activity

RNA extraction was carried out on tibial tissues from TM-infected and control mice for quantitative PCR. TM infection was associated with a notable upregulation of osteoclast-related gene expression, comprising Ctsk, FOS, NFATc1, and TRAP ($p < 0.05$) (Figure 3A–D). In addition, BMMs were obtained from the tibial bone marrow chamber and stimulated with RANKL to promote their differentiation into mature osteoclasts. TRAP staining demonstrated a pronounced rise in osteoclast number in the TM group relative to controls (Figure 3E). Phalloidin staining further confirmed enhanced formation of large, multinucleated, F-actin-positive osteoclasts in the TM group, indicating elevated bone-resorptive activity (Figure 3F).

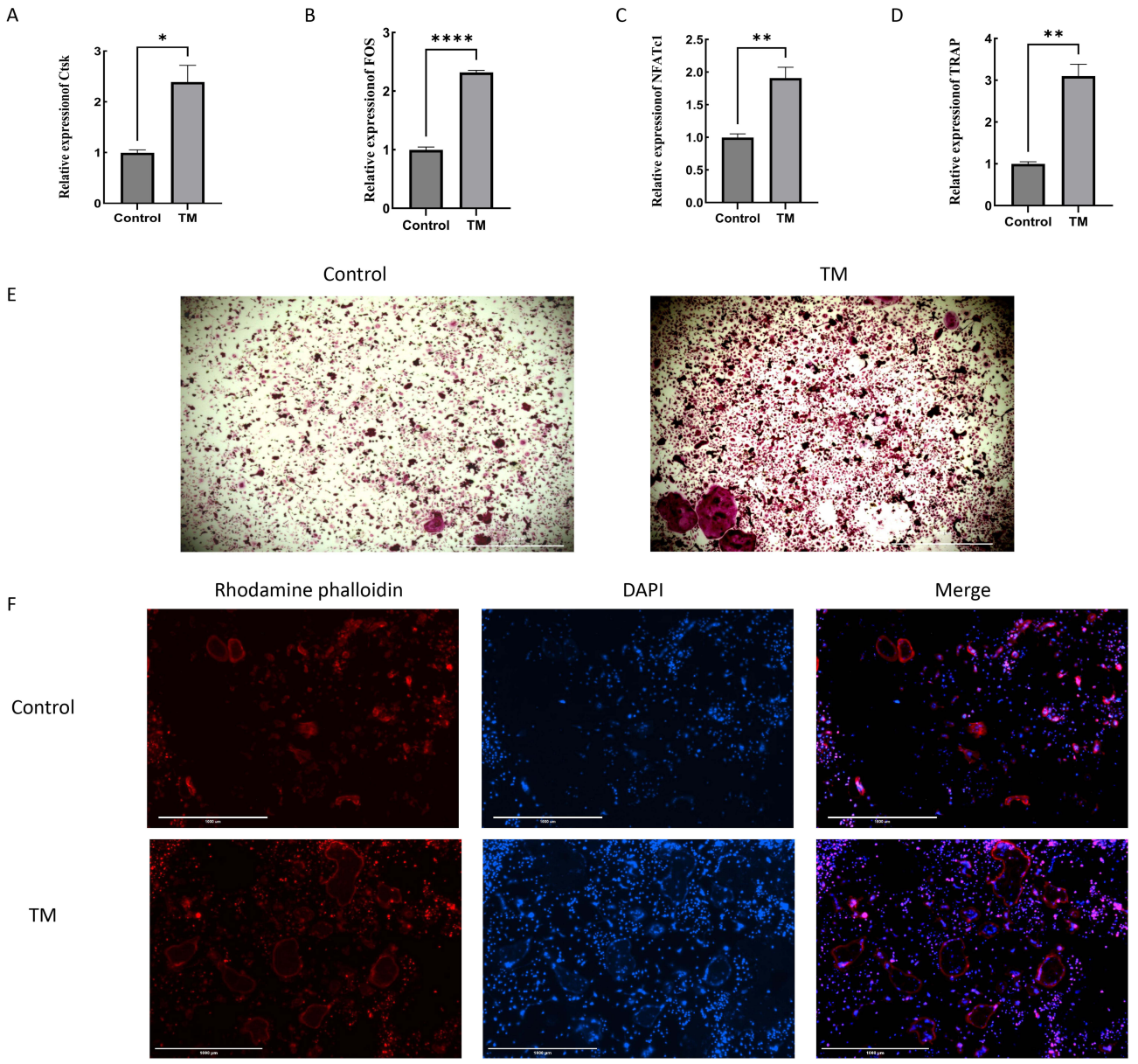

Figure 3 TM infection enhances osteoclast-related gene expression and promotes osteoclast formation. (**A**–**D**) qPCR analysis showing significantly elevated expression levels of osteoclast markers (**A**) Ctsk, (**B**) FOS, (**C**) NFATc1, and (**D**) TRAP in tibial tissue of TM-infected mice (normalized to β-actin). *$p < 0.05$, **$p < 0.01$, ****$p < 0.0001$ vs Control group. (**E**) TRAP staining of BMM-derived osteoclasts indicates increased osteoclast numbers in the TM group. (**F**) Phalloidin staining shows enhanced F-actin ring formation and multinucleation in osteoclasts from TM-infected mice.

Transcriptomic Profiling Reveals COMMD1 Downregulation and Activation of Osteoclastogenic Pathways

To investigate transcriptomic changes following TM infection, tibial bone tissue samples from mice were subjected to RNA sequencing. The volcano plot illustrated a marked downregulation of COMMD1 expression in the TM-infected group (Figure 4A). KEGG and GO analyses of DEGs showed significant enrichment in immune and inflammatory pathways, notably the NF-κB signaling cascade (Figure 4B–E). The heatmap illustrated elevated levels of osteoclast-related genes, including NFATc1 and TRAP, in the TM group relative to controls (Figure 4F).

https://doi.org/10.2147/IDR.S544816

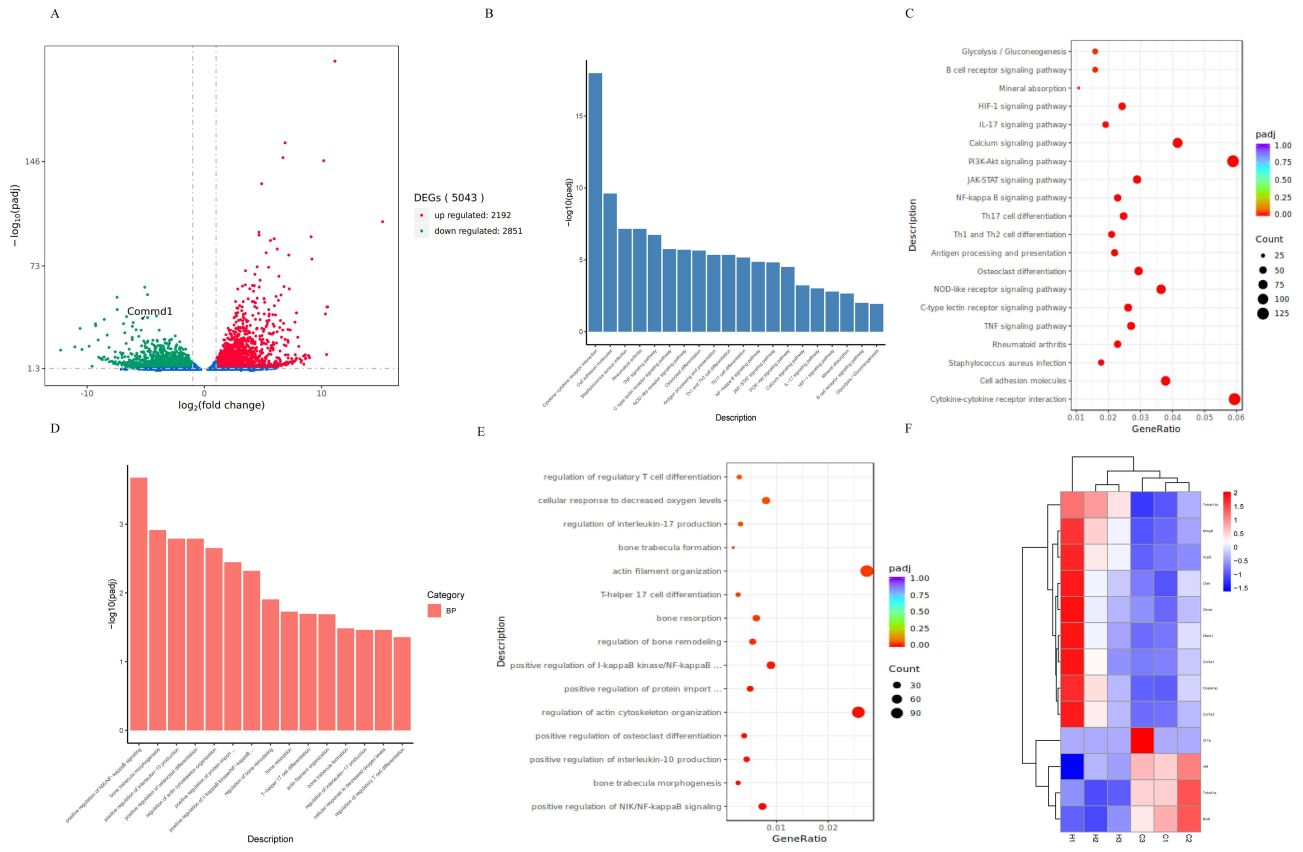

Figure 4 Transcriptomic analysis reveals COMMD1 downregulation and enrichment of osteoclast-related pathways in TM-infected tibiae. (**A**) Volcano plot showing differentially expressed genes; COMMD1 is significantly downregulated. (**B–E**) GO and KEGG enrichment analyses highlight involvement of NF-κB and osteoclast differentiation-related pathways. (**F**) Heatmap showing upregulation of osteoclast-related genes (NFATc1, TRAP, etc.) in the TM group.

COMMD1 Deletion Exacerbates TM-Induced Bone Destruction and Mechanical Weakening

To assess the role of COMMD1 in TM-induced bone damage, both wild-type (TM group) and COMMD1 conditional knockout mice (TM+cKO group) were infected with TM. Micro-CT imaging revealed more severe bone destruction and trabecular deterioration in the TM+cKO group relative to the TM group (Figure 5A). Quantitative assessment supported this finding this observation: TM+cKO mice exhibited significantly reduced bone volume fraction (BV/TV), bone volume (BV), and trabecular number (Tb.N), along with increased trabecular separation (Tb.Sp) ($p < 0.05$) (Figure 5B).

Histological examination with H&E and TRAP staining demonstrated enhanced inflammatory infiltration and bone loss in the TM+cKO group, characterized by markedly reduced or even absent trabeculae and obvious trabecular fusion, compared to the TM group (Figure 5C and D).

Biomechanical testing showed that the TM+cKO group had significantly lower elastic modulus, fracture-point force, and maximum bending stress, indicating compromised bone strength ($p < 0.05$) (Figure 5E). During the compression test, both stiffness (elastic modulus) and maximum stress were significantly diminished in the TM+cKO group as opposed to the TM group ($p < 0.05$) (Figure 5F).

COMMD1 Deficiency Enhances Osteoclast Differentiation in TM-Infected Mice

To assess the effect of COMMD1 deletion on osteoclast differentiation, RNA was extracted from tibial tissues of TM and TM+cKO mice for qPCR analysis. Compared with the TM group, the TM+cKO group exhibited a marked upregulation of osteoclast-related genes, including FOS, Ctsk, NFATc1, and TRAP ($p < 0.05$) (Figure 6A).

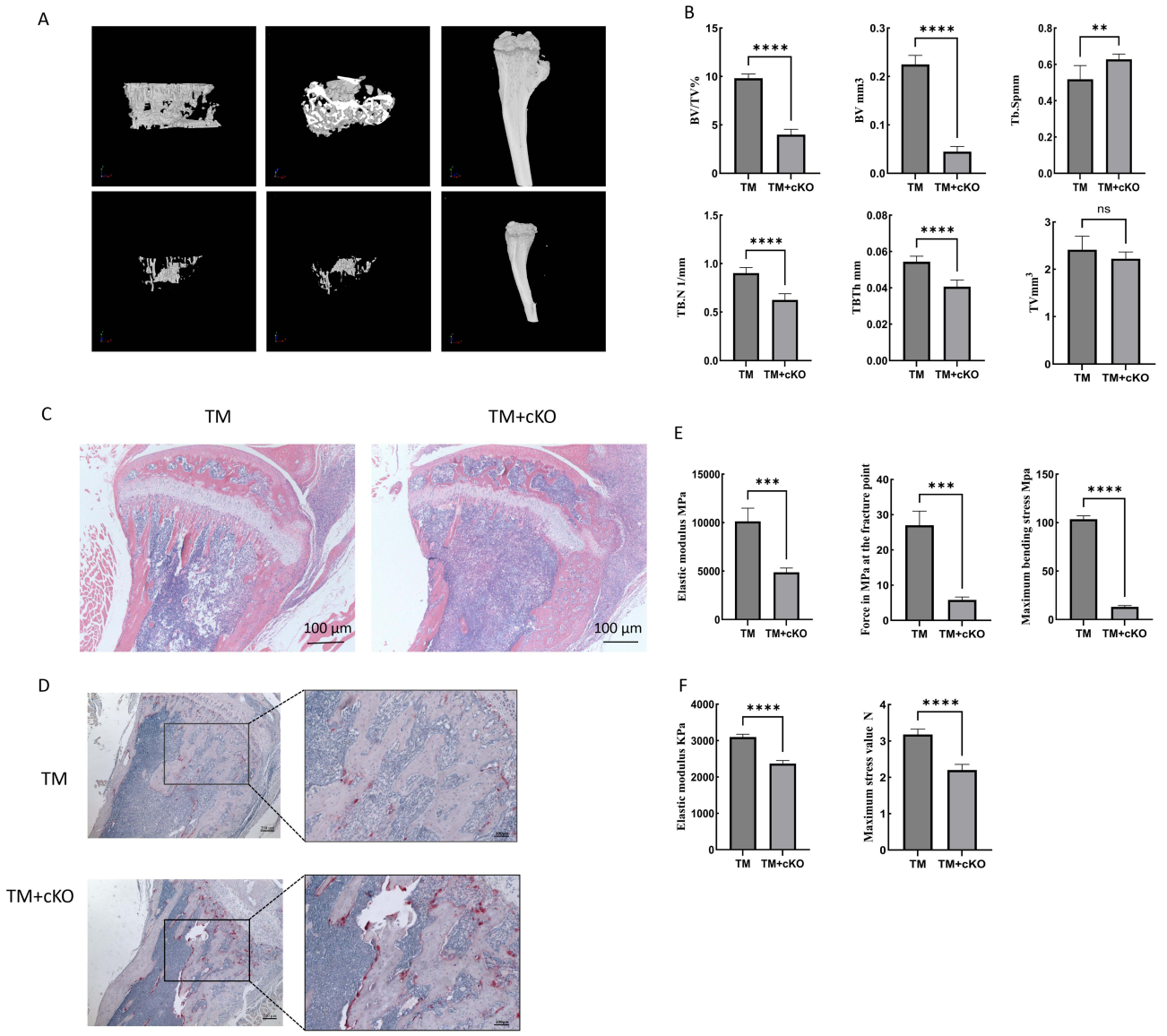

Figure 5 COMMD1 deletion exacerbates TM-induced bone destruction and mechanical weakening. (**A**) Micro-CT imaging shows more severe bone damage in TM+cKO mice than TM controls (x: left–right; y: anterior–posterior; z: superior–inferior) in micro-CT analysis). (**B**) Quantitative analysis of bone parameters shows decreased BV/TV, BV, Tb.N, and Tb.Th, with increased Tb.Sp in TM+cKO mice. (**C**) H&E staining indicates aggravated trabecular loss and inflammatory cell infiltration in the TM+cKO group. (**D**) TRAP staining shows increased osteoclast activity in TM+cKO tibiae. (**E**) Three-point bending tests reveal reduced elastic modulus, fracture-point force, and maximum bending stress. (**F**) Compression testing demonstrates significantly lower compressive modulus and maximum load in the TM+cKO group. n=5. $^{**}p < 0.01$, $^{***}p < 0.001$ vs TM-infected group.

Furthermore, BMMs isolated from both groups were subjected to TRAP and phalloidin staining. The TM+cKO group showed a markedly higher number of large, multinucleated, more F-actin–labeled osteoclasts than observed in the TM group (Figure 6B and C), indicating that COMMD1 deficiency promotes osteoclastogenesis during TM infection.

COMMD1 Influences Osteoclast Differentiation Through the NF-κB Signaling Pathway

First, the protein manifestation of COMMD1 in BMMs was verified. COMMD1 expression in BMMs showed a notable reduction in cKO mice when compared with controls ($p < 0.05$) (Figure 7A). Next, BMMs from different groups were infected with TM for 7 days, and osteoclast-related proteins and NF-κB signaling pathway proteins were analyzed. It was shown that loss of COMMD1 led to a pronounced enhancement in osteoclast-related protein expression ($p < 0.05$) (Figure 7B). Notably, a significant elevation in P-P65 and a reduction in IκBα were detected ($p < 0.05$) (Figure 7C).

https://doi.org/10.2147/IDR.S544816

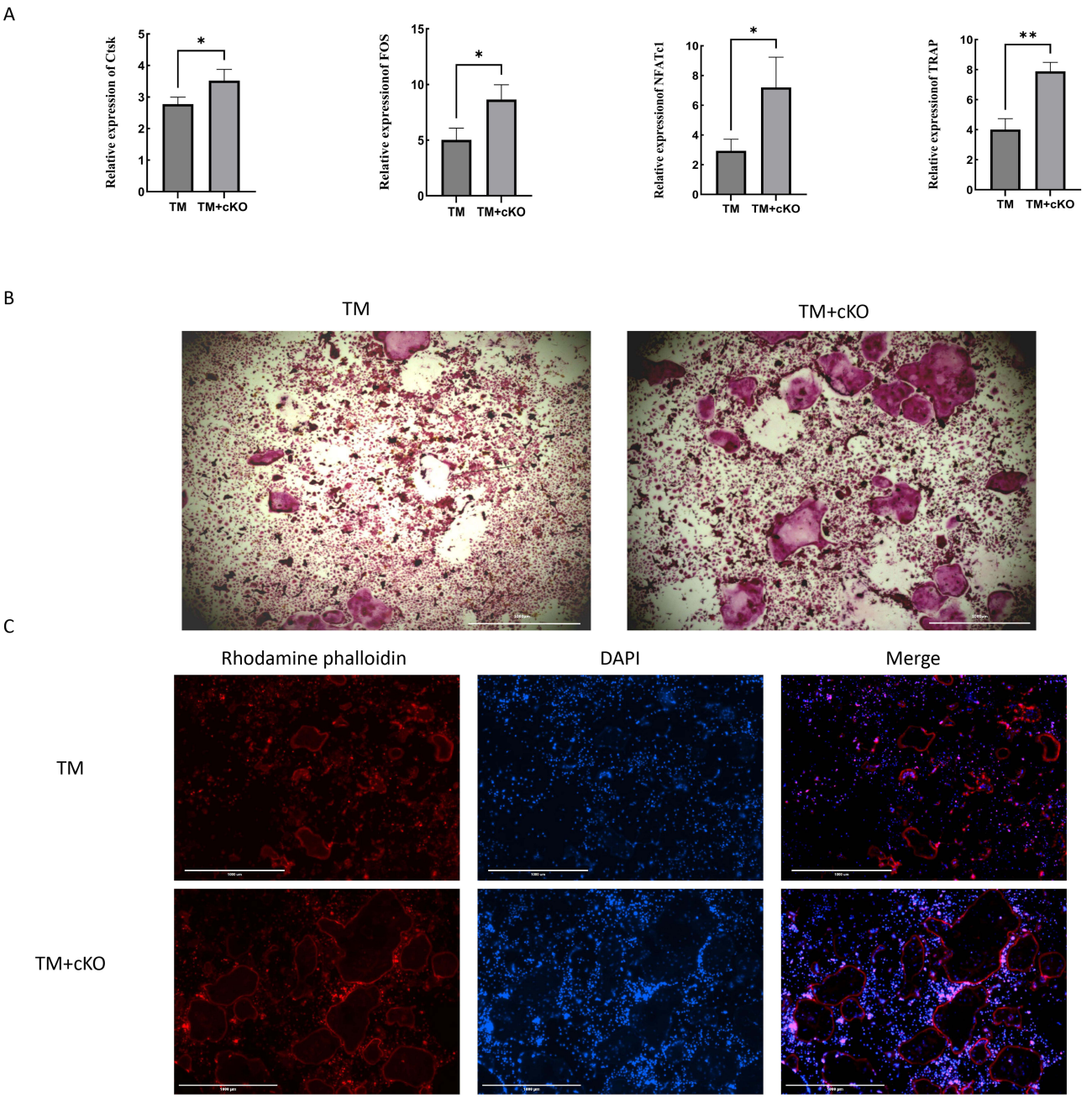

Figure 6 COMMD1 deficiency enhances osteoclast differentiation in TM-infected mice. (**A**) qPCR analysis shows increased expression of Ctsk, FOS, NFATc1, and TRAP in the TM+cKO group (normalized to β-actin). *$p < 0.05$, **$p < 0.01$ vs TM-infected group. (**B**) TRAP staining reveals more numerous and larger osteoclasts in the TM+cKO group. (**C**) Phalloidin staining shows enhanced F-actin ring formation and multinucleation in the TM+cKO group.

To better understand how COMMD1 regulates osteoclast differentiation, BMMs were transfected with a plasmid to overexpress COMMD1 ($p < 0.05$) (Figure 7D). Under TM stimulation, COMMD1-OE significantly suppressed NFATc1, Ctsk, and FOS, and attenuated NF-κB activation—evidenced by decreased P-P65/P65 and increased IκBα—compared with TM alone (all $p < 0.05$) (Figures 7E–F).

Furthermore, to verify whether the NF-κB signaling pathway participates in COMMD1-regulated osteoclast differentiation, BMMs were exposed to the specific inhibitor JSH-23. JSH-23 was found to markedly reduce the levels of osteoclast-associated proteins in BMMs derived from cKO mice under TM-infected conditions. ($p < 0.05$) (Figure 7G), further supporting the conclusion that COMMD1 modulates NF-κB-dependent osteoclast differentiation.

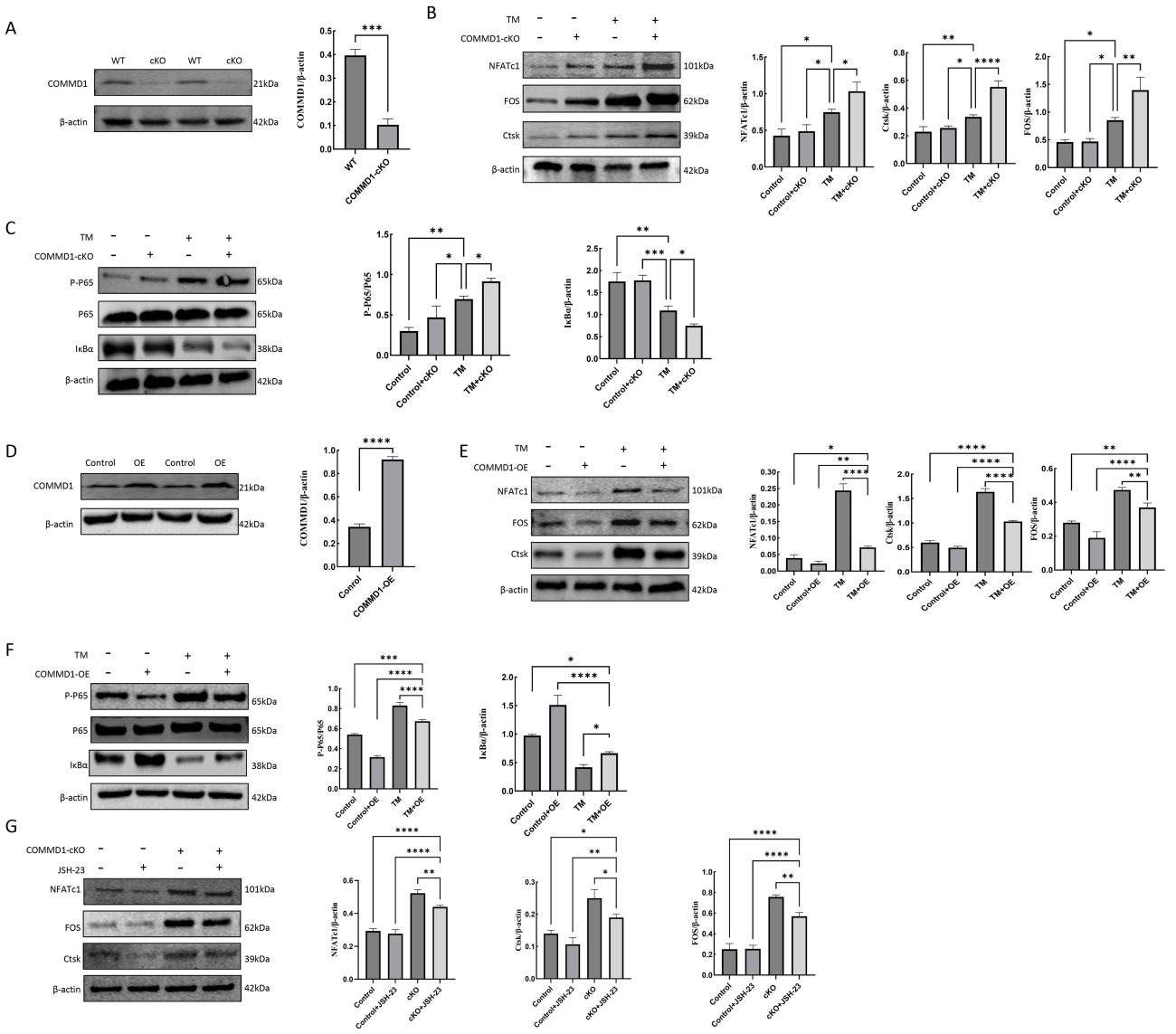

Figure 7 COMMD1 regulates osteoclastogenesis via the NF-κB signaling pathway. (**A**) Western blot analysis confirming COMMD1 expression in BMMs from the mice. (**B**) Increased expression of osteoclast markers (NFATc1, Ctsk, FOS) in cKO-derived BMMs under TM treatment. (**C**) P-P65 and IκBα expression in COMMD1-cKO BMMs after TM treatment. (**D**) Verification of COMMD1 overexpression efficiency in BMMs (**E**) COMMD1 overexpression suppresses osteoclast marker expression, (**F**) COMMD1 overexpression reduces P-P65 levels and increases IκBα expression following TM infection. (**G**) NF-κB inhibitor JSH-23 reduces osteoclast-related protein expression in cKO-derived BMMs under TM infection. *$p < 0.05$, **$p < 0.01$, ***$p < 0.001$, ****$p < 0.0001$.

Discussion

OM refers to a bone condition initiated by the invasion of microbial pathogens, which ultimately causes progressive degradation of bone tissue.[25] The majority of pathological features in OM are linked to skeletal destruction and impairment, caused by a disturbance in the equilibrium between osteoblasts and osteoclasts throughout bone remodelling.[26] Staphylococcus aureus (S. aureus) is considered the primary contributor to OM.[27] However, fungi and viruses can also lead to OM. TM commonly presents with lung and skin lesions and has recently been associated with OM cases.[16,28] In this study, TM was used to simulate the microbial source of infection in OM. Subsequent to TM application, significant osteoclast activity was noted in the TM-treated group, as indicated by a substantial increase in TRAP-stained osteoclasts, clear fusion of bone trabeculae in H&E staining, and a marked rise in osteoclast-related markers. In summary, these data suggested that TM infection significantly enhanced osteoclast differentiation.

https://doi.org/10.2147/IDR.S544816

COMMD1 is a multifunctional regulatory protein engaged in various biological functions, such as copper homeostasis, protein degradation, and inflammatory responses.[17,29,30] It has also been implicated in immune-related diseases and tumorigenesis.[31,32] According to previous reports, COMMD1 is closely attributed to osteoclast function in rheumatoid arthritis, and its altered expression may influence bone resorption, suggesting a possible involvement in bone metabolism.[20] In our study, RNA-seq analysis of TM-infected bone tissue in a murine OM model revealed significantly reduced COMMD1 expression in infected bone tissue. Subsequent in vitro and in vivo experiments demonstrated that COMMD1 scarcity promoted osteoclast differentiation and exacerbated bone destruction, whereas COMMD1 overexpression suppressed osteoclast marker expression and alleviated bone damage. These findings indicate that COMMD1 may exert a protective role in TM-induced OM by regulating osteoclast differentiation. The specific molecular mechanisms responsible for this regulatory activity are still unclear. NF-κB serves as a pivotal modulator of immune and inflammatory activities and is essential for sustaining bone metabolic equilibrium, particularly by serving as a key regulator in osteoclast differentiation and activation.[33,34] The classical RANK/RANKL signaling axis activates the IKK complex, causing the breakdown of IκBα followed by the release of NF-κB subunits, such as P65. This process promotes the transcriptional activation of downstream target genes, including NFATc1, TRAP, and Ctsk, thereby driving osteoclast maturation.[35,36] Recent evidence suggests that RANKL promotes the generation of super-enhancers (SEs) and their associated eRNAs, which drive the epigenetic reprogramming of human macrophages into osteoclasts. NF-κB acts as an early signaling mediator in this process, initiating the expression of key transcription factors and priming the chromatin landscape for subsequent SE-driven transcriptional activation.[37]

Although the involvement of NF-κB in various bone-destructive diseases has been extensively studied, its specific role in fungal infection-induced osteomyelitis remains unclear, with limited research focusing on TM-associated cases. In our study, RNA sequencing analysis indicated significant induction of NF-κB signaling in TM-associated osteomyelitis Further in vitro experiments demonstrated that COMMD1 deficiency markedly increased the phosphorylation level of P65, whereas COMMD1 overexpression led to a reduction in P-P65 levels, this suggests a potential role for COMMD1 in NF-κB-dependent osteoclastogenesis.[20] The observed downregulation of osteoclast-related proteins following JSH-23 treatment provides additional evidence that COMMD1 participates in TM-driven osteoclast differentiation by modulating NF-κB signaling. This research has several limitations. First, although we demonstrated that COMMD1 modulates osteoclastogenesis through NF-κB signaling, its potential crosstalk with other signaling pathways remains to be explored. Second, the findings are primarily based on a murine model and in vitro experiments; further validation using clinical samples is needed to assess the relevance of COMMD1 in human osteomyelitis.

Conclusion

A systematic investigation was conducted to clarify the role and regulatory function of COMMD1 in TM-triggered OM. Using a murine model of TM infection, we displayed that the pathogen causes significant bone structural damage and mechanical weakening, accompanied by enhanced osteoclast activity and upregulation of osteoclast-related genes. Further in vitro and in vivo studies demonstrated that COMMD1 deficiency aggravated bone destruction and promoted osteoclast formation, whereas COMMD1 overexpression effectively suppressed these effects. Mechanistically, COMMD1 deficiency led to triggering of the NF-κB pathway. Overall, our unearthing highlight the protective role of COMMD1 in TM-induced OM, chiefly via downregulation of osteoclast formation and function, mediated by blockade of the NF-κB pathway. Future studies should further investigate the crosstalk between COMMD1 and other key signaling pathways in fungal osteomyelitis and validate these findings in clinical samples to assess their relevance and translational potential in human disease.

Data Sharing Statement

The data used to support the findings of this study are available from the corresponding author upon request (E-mail: zongshaohui@gxmu.edu.cn).

Ethical Statement

This study has been approved by the Animal Ethics Committee of Guangxi Medical University (NO. 202210014) and conducted in compliance with the institutional guidelines (Directive 2010/63/EU in Europe) for the care and use of animals.

Author Contributions

All authors made a significant contribution to the work reported, whether that is in the conception, study design, execution, acquisition of data, analysis and interpretation, or in all these areas; took part in drafting, revising or critically reviewing the article; gave final approval of the version to be published; have agreed on the journal to which the article has been submitted; and agree to be accountable for all aspects of the work.

Funding

This study was supported by National Natural Science Foundation of China (82260437).

Disclosure

The authors declare that there are no conflicts of interest regarding the publication of this paper.

References

1. Kavanagh N, Ryan EJ, Widaa A, et al. Staphylococcal osteomyelitis: disease progression, treatment challenges, and future directions. *Clin Microbiol Rev*. 2018;31(2). doi:10.1128/CMR.00084-17
2. McLeod N, Fisher M, Lasala PR. Vertebral osteomyelitis due to Candida species. *Infection*. 2019;47(3):475–478. doi:10.1007/s15010-019-01294-6
3. Sun Z, Ji J, Zuo L, et al. Causal relationship between nonalcoholic fatty liver disease and different sleep traits: a bidirectional Mendelian randomized study. *Front Endocrinol*. 2023;14:1159258. doi:10.3389/fendo.2023.1159258
4. Hofstee MI, Muthukrishnan G, Atkins GJ, et al. Current concepts of osteomyelitis: from pathologic mechanisms to advanced research methods. *Am J Pathol*. 2020;190(6):1151–1163. doi:10.1016/j.ajpath.2020.02.007
5. Fantoni M, Taccari F, Giovannenze F. Systemic antibiotic treatment of chronic osteomyelitis in adults. *Eur Rev Med Pharmacol Sci*. 2019;23(2 Suppl):258–270. doi:10.26355/eurrev_201904_17500
6. Chang RYK, Nang SC, Chan HK, Li J. Novel antimicrobial agents for combating antibiotic-resistant bacteria. *Adv Drug Deliv Rev*. 2022;187:114378. doi:10.1016/j.addr.2022.114378
7. Wassif RK, Elkayal M, Shamma RN, Elkheshen SA. Recent advances in the local antibiotics delivery systems for management of osteomyelitis. *Drug Deliv*. 2021;28(1):2392–2414. doi:10.1080/10717544.2021.1998246
8. Salman R, McGraw M, Naffaa L. Chronic osteomyelitis of long bones: imaging pearls and pitfalls in pediatrics. *Semin Ultrasound CT MR*. 2022;43(1):88–96. doi:10.1053/j.sult.2021.05.009
9. Shen Q, Sheng L, Zhang J, Ye J, Zhou J. Analysis of clinical characteristics and prognosis of talaromycosis (with or without human immunodeficiency virus) from a non-endemic area: a retrospective study. *Infection*. 2022;50(1):169–178. doi:10.1007/s15010-021-01679-6
10. Guo J, Ning XQ, Ding JY, et al. Anti-IFN-gamma autoantibodies underlie disseminated Talaromyces marneffei infections. *J Exp Med*. 2020;217(12). doi:10.1084/jem.20190502
11. Tsang CC, Lau SKP, Woo PCY. Sixty years from segretain's description: what have we learned and should learn about the basic mycology of Talaromyces marneffei? *Mycopathologia*. 2019;184(6):721–729. doi:10.1007/s11046-019-00395-y
12. Yu L, Zhang B, Shi J, Wang M, Wan H. Osteoarticular infection caused by Talaromyces marneffei and Salmonella in a person living with HIV: a case report. *BMC Infect Dis*. 2023;23(1):560. doi:10.1186/s12879-023-08554-9
13. Moni BM, Wise BL, Loots GG, Weilhammer DR. Coccidioidomycosis Osteoarticular Dissemination. *J Fungi*. 2023;9(10):1002. doi:10.3390/jof9101002
14. Benchbani H, Mallett K, Warady BA, Ahmed AA. Histoplasma osteomyelitis in a 15-year-old kidney transplant patient. *Transpl Infect Dis*. 2022;24(6):e13953. doi:10.1111/tid.13953
15. McCabe MP, Heck RK. Histoplasma osteomyelitis simulating giant-cell tumor of the distal part of the radius: a case report. *J Bone Joint Surg Am*. 2010;92(3):708–714. doi:10.2106/JBJS.H.01507
16. Liu GN, Huang JS, Zhong XN, et al. Penicillium marneffei infection within an osteolytic lesion in an HIV-negative patient. *Int J Infect Dis*. 2014;23:1–3. doi:10.1016/j.ijid.2013.12.019
17. Weiskirchen R, Penning LC. COMMD1, a multi-potent intracellular protein involved in copper homeostasis, protein trafficking, inflammation, and cancer. *J Trace Elem Med Biol*. 2021;65:126712. doi:10.1016/j.jtemb.2021.126712
18. Wang X, He S, Zheng X, et al. Transcriptional analysis of the expression, prognostic value and immune infiltration activities of the COMMD protein family in hepatocellular carcinoma. *BMC Cancer*. 2021;21(1):1001. doi:10.1186/s12885-021-08699-3
19. Yeh DW, Chen YS, Lai CY, et al. Downregulation of COMMD1 by miR-205 promotes a positive feedback loop for amplifying inflammatory- and stemness-associated properties of cancer cells. *Cell Death Differ*. 2016;23(5):841–852. doi:10.1038/cdd.2015.147
20. Murata K, Fang C, Terao C, et al. Hypoxia-sensitive COMMD1 integrates signaling and cellular metabolism in human macrophages and suppresses osteoclastogenesis. *Immunity*. 2017;47(1):66–79e65. doi:10.1016/j.immuni.2017.06.018
21. Wang Y, Zhang B, Fan F, et al. COMMD3 regulates copper metabolism via the ATOX1-ATP7A-LOX axis to promote multiple myeloma progression. *Biomedicines*. 2025;13(2):351.

22. Zhang Y, Wang Z, Xie X, et al. Tatarinan N inhibits osteoclast differentiation through attenuating NF-kappaB, MAPKs and Ca(2+)-dependent signaling. *Int Immunopharmacol*. 2018;65:199–211. doi:10.1016/j.intimp.2018.09.030
23. Xu X, Liu N, Wang Y, et al. Tatarinan O, a lignin-like compound from the roots of Acorus tatarinowii Schott inhibits osteoclast differentiation through suppressing the expression of c-Fos and NFATc1. *Int Immunopharmacol*. 2016;34:212–219. doi:10.1016/j.intimp.2016.03.001
24. Feng Y, Zhou M, Zhang Q, et al. Synergistic effects of high dietary calcium and exogenous parathyroid hormone in promoting osteoblastic bone formation in mice. *Br J Nutr*. 2015;113(6):909–922. doi:10.1017/S0007114514004309
25. Lan Y, Xie H, Shi Y, et al. NEMO-binding domain peptide ameliorates inflammatory bone destruction in a Staphylococcus aureus-induced chronic osteomyelitis model. *Mol Med Rep*. 2019;19(4):3291–3297. doi:10.3892/mmr.2019.9975
26. Wang X, Zheng R, Huang X, et al. Effects of alkaloids from Sophora flavescens on osteoblasts infected with Staphylococcus aureus and osteoclasts. *Phytother Res*. 2018;32(7):1354–1363. doi:10.1002/ptr.6069
27. Paolella F, Gabusi E, Manferdini C, Schiavinato A, Lisignoli G. Specific concentration of hyaluronan amide derivative induces osteogenic mineralization of human mesenchymal stromal cells: evidence of RUNX2 and COL1A1 genes modulation. *J Biomed Mater Res A*. 2019;107 (12):2774–2783. doi:10.1002/jbm.a.36780
28. Li HR, Cai SX, Chen YS, et al. Comparison of Talaromyces marneffei infection in human immunodeficiency virus-positive and human immunodeficiency virus-negative patients from Fujian, China. *Chin Med J*. 2016;129(9):1059–1065. doi:10.4103/0366-6999.180520
29. Riera-Romo M. COMMD1: a multifunctional regulatory protein. *J Cell Biochem*. 2017;119(1):34–51. doi:10.1002/jcb.26151
30. Fedoseienko A, Bartuzi P, van de Sluis B. Functional understanding of the versatile protein copper metabolism MURR1 domain 1 (COMMD1) in copper homeostasis. *Ann N Y Acad Sci*. 2014;1314:6–14. doi:10.1111/nyas.12353
31. Mu P, Akashi T, Lu F, Kishida S, Kadomatsu K. A novel nuclear complex of DRR1, F-actin and COMMD1 involved in NF-kappaB degradation and cell growth suppression in neuroblastoma. *Oncogene*. 2017;36(41):5745–5756. doi:10.1038/onc.2017.181
32. Li H, Chan L, Bartuzi P, et al. Copper metabolism domain-containing 1 represses genes that promote inflammation and protects mice from colitis and colitis-associated cancer. *Gastroenterology*. 2014;147(1):184–195e183. doi:10.1053/j.gastro.2014.04.007
33. Lin T-H, Tamaki Y, Pajarinen J, et al. Chronic inflammation in biomaterial-induced periprosthetic osteolysis: NF-κB as a therapeutic target. *Acta Biomater*. 2014;10(1):1–10. doi:10.1016/j.actbio.2013.09.034
34. Zhang Y, Ma C, Liu C, Wu W. NF-kappaB promotes osteoclast differentiation by overexpressing MITF via down regulating microRNA-1276 expression. *Life Sci*. 2020;258:118093. doi:10.1016/j.lfs.2020.118093
35. Crockett JC, Mellis DJ, Scott DI, Helfrich MH. New knowledge on critical osteoclast formation and activation pathways from study of rare genetic diseases of osteoclasts: focus on the RANK/RANKL axis. *Osteoporos Int*. 2011;22(1):1–20. doi:10.1007/s00198-010-1272-8
36. Zeng XZ, He LG, Wang S, et al. Aconine inhibits RANKL-induced osteoclast differentiation in RAW264.7 cells by suppressing NF-κB and NFATc1 activation and DC-STAMP expression. *Acta Pharmacol Sin*. 2016;37:255–263. doi:10.1038/aps.2015.85
37. Bae S, Kim K, Kang K, et al. RANKL-responsive epigenetic mechanism reprograms macrophages into bone-resorbing osteoclasts. *Cell Mol Immunol*. 2023;20(1):94–109. doi:10.1038/s41423-022-00959-x